Development and testing of a novel tri-rotor configuration for application in a fixed wing VTOL aircraft

António Augusto Lopes do Arco
antonio.arco@tecnico.ulisboa.pt

Instituto Superior Técnico, Universidade de Lisboa, Portugal

December 2022

Abstract

The versatility of vertical take-off and landing (VTOL) aircraft has led to an increase in demand for new configurations of such vehicles, namely for Urban Air Mobility and military applications. For the later, VTOL systems are particularly interesting when applied to Unmanned Aerial Vehicles (UAVs), allowing for their deployment irrespective of location and existent infrastructure. In this thesis, a new configuration of tri-rotor aircraft is presented and the proof of concept of hovering and forward flight capabilities pursued, as to determine the airworthiness of such configuration and the feasibility of applying it to a future, fixed wing, VTOL UAV. First, the flight dynamics model (FDM) of the vehicle configuration was deduced, a Simulink controller designed, and parametric studies conducted to determine the trim conditions in hover. Later, a PX4 autopilot was obtained and tuned. Then, the test vehicle was designed, with particular focus on the tilting mechanisms of the front and rear rotors, which were tested to access their performance and map their actuation. A study on the loss of efficiency ($\sim 19\%$ in hover) arising from introducing a gearbox in the rear rotor system was performed. After this, a sequence of flight tests which lead to the proof of concept was performed, as well as additional flights for data collection. Finally, two system identification methods (time-based and frequency-response approaches) were used to obtain dynamic models capable of replicating a validation flight. The first approach managed to replicate $2s$ of the flight while the later managed to replicate it entirely.

Keywords: Vertical Take-Off and Landing, Unmanned Aerial Vehicle, Novel configuration, Flight Dynamics Model, System Identification

1. Introduction

1.1. Motivation, Project Overview and Requirements

One of the hottest topics in the current aerospace engineering paradigm is the development of hybrid configuration aircraft which combine the horizontal flight efficiency of a fixed wing aircraft with the flexibility of performing VTOL and steady hovering manoeuvres that was until recently reserved for rotary wing vehicles such as helicopters and multicopters. With the advent of Urban Air Mobility and the increasing demand, specially by the military, of primarily unmanned aircraft which incorporate the aforementioned characteristics, investigation on the development of novel configurations of VTOL aircraft designs presents an unprecedented level of relevance.

Nevertheless, aircraft design is still a complex task which often relies on the creativity of the designers to obtain new strategies that allow to push the boundaries of aircraft efficiency and versatility to new levels. As so, the main goal of this work is to perform the proof of concept of a ground breaking multi-rotor design that, when applied to an already existent aircraft, will allow for the optimization of its aerodynamic characteristics when in fixed wing mode, while equipping it with the versatility of a VTOL vehicle through the use of thrust vectoring.

After designing, building and flying a test vehicle, and once the airworthiness of the concept is proved, the secondary objective of this work is to apply two system identification (SID) methodologies to the data collected during flight testing and further improve the FDM initially developed.

This project is part of the larger Mini-E project which is currently in development at the Center for Aerospace Research of the University of Victoria (CfAR) through a partnership with the Defense Research and Development Canada (DRDC). Such aircraft is being designed with the ultimate purpose of performing surveillance flights carrying a Magnetic Anomaly Detection sensor (MAD-XR) to detect magnetic anomalies occurring at sea, such as manned submarines or other underwater ROVs (Remotely Operated Vehicles). Since the primary use of this aircraft will be in maritime environment,

being deployed from ships, one of the most critical aspects of its design is the requirement of being able to perform VTOL manoeuvres while also maximizing the aircraft's range.

Similarly to the fixed wing design (Figure 1), where the main wing was designed to carry around 80% of the aircraft's weight in cruise conditions while the canard holds the remaining 20%, so does the VTOL system present such weight distribution, with the frontal rotors being responsible for providing a thrust that accounts for 10% of the overall aircraft's weight each while the rear rotor, which will also be providing thrust in horizontal flight, will be responsible for developing 80% of the thrust required to hover. The rear rotor, with its dual purpose, will present a pusher configuration in horizontal flight and a fully upright position in the vertical stints of the mission, thus requiring a custom tilting mechanism to be developed. Furthermore, this tilting mechanism should be designed in a way that it ensures that the motor itself remains fixed throughout the entire operation of the aircraft since in its final version the rear rotor will be powered by an Internal Combustion Engine. The tilting action of the rear rotor will also be used to perform the transition of the aircraft between vertical and horizontal flight conditions, a task that will also be addressed in this investigation.

Meanwhile, the front rotors shall be powered, in all versions, by electric motors, in a way that the final aircraft will most likely present an hybrid propulsion system. These rotors will also be required to tilt in an effort to obtain the thrust vectoring necessary to stabilize this multi-rotor aircraft in vertical flight conditions, thus requiring the design of a second (front) tilting mechanism.

2. Theoretical Background

2.1. Flight Dynamics Model

The characterization of an aircraft's dynamics usually includes some underlying assumptions, namely that the vehicle's body presents y-symmetry and that both its mass and inertia tensor are constant. This later assumption is particularly truthful when dealing with electric vehicles as will be the case of the test vehicle designed in this work for proof of concept purposes. Such studies usually start with the derivation of the dynamic equations for linear (1) and angular momentum (2) from the Newton-Euler equations.

$$F_t = m\left(\frac{d}{dt}V + \omega \times V\right) \tag{1}$$

$$M_t = I_b\left(\frac{d}{dt}\omega + \omega \times \omega\right) \tag{2}$$

F_t and M_t represent, respectively, the summation of all the forces and moments acting upon the body. F_t includes the contributions of gravity, aerodynamic forces acting upon the aircraft's body and of the propulsive forces generated by the rotors. Meanwhile, M_t accounts for the aerodynamic moments and for the torques that are associated with not only the thrust generated by the rotating propellers in combination with their distance to the aircraft's CG but also with the aerodynamic drag that arises from this rotational motion (drag torque).

2.2. Gearbox Efficiency

Gearboxes are indispensable in many applications where the transmission and manipulation of mechanical power is required, whether these imply a change in torque/rotational speed between axis or the transmission of power between axis which are not aligned between them. However, as in any system, gearboxes present losses, particularly due to friction. The relation between the mechanical efficiency (η) of a two gear system and the friction coefficient verified between the teeth surfaces (f) [1] can be given by:

$$\eta = 1 - \frac{f}{2\cos\alpha}\left(\frac{1}{R_1} \pm \frac{1}{R_2}\right)\frac{l_a^2 + l_f^2}{l_a + l_f} \tag{3}$$

Several researchers have verified the general trend of increasing gearbox efficiency with the applied load [2–8], with this phenomenon being usually attributed to the reduction in the friction coefficient that is registered for increasing loading and teeth sliding speed conditions [9, 10].

2.3. System Identification

Dynamic models can either be obtained through the development of a physical FDM or through the use of system identification techniques. These two options present themselves as alternative but also complementary FDM development strategies, particularly in the initial stages of aircraft development. SID techniques can be applied not only to the entire aircraft system but also to individual components such as the actuators. This is particularly relevant in the initial stage of the development of a physics based FDM where the use of SID generated models for the actuators for example can help reduce the number and extension of the assumptions that are made, thus enhancing the resemblance of the designed model to the one of the real vehicle.

Moreover, when applied to the entire vehicle, SID techniques allow to obtain a complete model which describes the dynamics of the vehicle as a whole and not as a related group of individual modulus. This poses and advantage against the physics based model, where the aircraft's dynamics are divided in subsystems (eg.: aerodynamics, structural behaviour, ...) which are then related amongst them by an additional set of assumptions.

System identification methods can be divided into parametric and non-parametric with the first category involving all of the techniques which return numerical values for defined parameters. Such techniques can be used when a preliminary, physics based, FDM already exists and the objective is to enhance its fitment to a set of test data or when one aims to obtaining, for example, a transfer-function based model which describes the relation between a specific set of inputs and outputs. Non-parametric methods allow to obtain models which enclose the key aspects of the dynamics of the vehicle without providing intelligible values. These are usually referred to as "black-box" models. Furthermore, SID methods can be divided in time-based or frequency-response based, depending on the way the data is treated and the model developed, whether by adjusting the FDM in order for the simulated outputs to be as close to the real test ones as possible over time or as a function of the control input frequency, respectively.

In order to obtain the required data to perform system identification, test flights which include specific sets of manoeuvres must be conducted, in a way that only an already airworthy aircraft can be the subject of SID techniques. The most commonly used manoeuvres are the *doublets* and the *chirps* (or *frequency sweeps*).

3. Flight Dynamics Model

In order to gain an initial understanding on the expected dynamics of any novel configuration aircraft, a FDM has first to be derived. When it comes to the Mini-E aircraft, its horizontal flight dynamics have already been studied before by Diogo Tomás in [11] while the vertical flight dynamics have been addressed previously by Sara Pedro in [12] but for a more common, 50/50, quadrotor configuration. As so, a preliminary FDM needed to be derived for the proposed tri-rotor configuration and the dynamics of the conceptual vehicle studied before proceeding with the project.

The rotor numbering and nomenclature of some relevant distances (x_f, x_r and y_r) can be found in figure 1 while the definition of some important angular units related to the frontal arms operation such as the opening angle (Γ) and tilting angle (δ_{arms}) can be found in Figure 2.

These variables will be of paramount importance in the definition of the propulsive forces and moments equations. Additionally, an extra variable (μ) was used in the deduction of these equations in order to account for the tilting angle of the rear rotor.

3.1. Dynamics Equations

Unlike more conventional multi-rotor vehicles, which present slender airframes and where the influence of aerodynamic forces and moments on its dynamics are many times neglected, the same cannot be done in the case of a VTOL, fixed wing, aircraft. As so, it shall be considered that the aircraft is subjected to three types of forces - Aerodynamic, Propulsive and Gravitational - and also to the associated moments. Gyroscopic effects due to rotation of the rotors and the aircraft's change in attitude will also be considered. Equations 1 and 2 will then be manipulated as to account for such contributions.

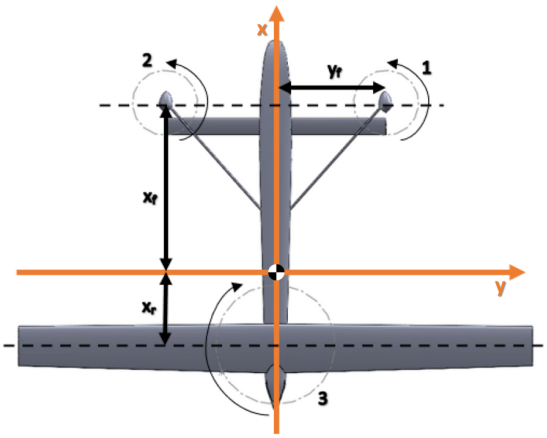

Figure 1: Tri-rotor configuration [12].

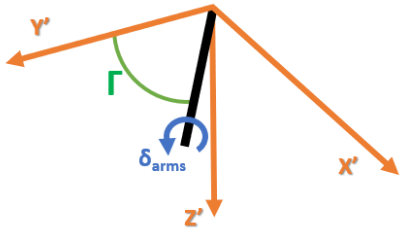

Figure 2: Right frontal arm rotation angles.

The preliminary definition of the propulsive forces and moments was done considering that the three rotors were contained in the same XY plane as the aircraft's center of gravity and that the dimensions depicted in Figure 1 were the ones shown on Table 1 for the case of the Mini-E aircraft.

Table 1: Rotor distances from the center of gravity of the Mini-E aircraft [12].

Distance [m]	
x_f	0.891
x_r	0.222
y_f	0.483

When it came to the definition of the influence of aerodynamics on the vehicle's dynamics, the usual equations [13] were considered to account for the

contributions of aerodynamic forces and moments to the overall dynamics of the vehicle and considering the aerodynamic constants and surface dimensions which were determined in [11].

However, a simplified aerodynamic model needed to be defined additionally for the test vehicle which would be later built in order to perform flight testing of the novel tri-rotor configuration presented, as this aircraft's body would take a rather different format than the Mini-E since it was designed as a simple multi-rotor without lifting surfaces. As so, and given the rather simplistic design of this vehicle's airframe, it was considered that the drag coefficient would be the one of a plane placed perpendicularly against an oncoming flow and the reference areas were defined according to a preliminary CAD model developed in parallel.

For the case of the contribution of the gravitational forces, the common expressions were employed, being no different in their definition than in any other common aircraft. The influence of gyroscopic effects on the overall dynamics is dependent of the rotors' inertial characteristics, rotational speed, sense of rotation, spatial orientation and on the angular rates of the entire vehicle's body at any given instant. The contributions of the gyroscopic moments to the overall model were therefore also accounted for.

The obtained equations were then linearized by applying the small perturbation theory around the equilibrium condition of steady hovering flight. However, the aerodynamic equations could not be linearized as in equilibrium the three components of the velocity would be zero. As so, the second order terms of the disturbances were considered exceptionally for the aerodynamic equations in order to account for the influence of gusts upon the vehicle's dynamics.

3.2. Controller

With the preliminary FDM defined and in order to gain an initial understanding on the expected behaviour of the proposed configuration while in hovering flight, a basic altitude and attitude controller was implemented in Simulink®. The controller was requested to maintain a fixed altitude while following null values of roll, pitch and yaw angles, with the main conclusion being that the aircraft could indeed assume such attitude at the expense of constantly drifting to the right due to the thrust vectoring happening in the front rotors, needed to maintain an equilibrium of torques along the yaw axis.

3.3. Trim Analysis and Parametric Studies

The next step in this investigation was then to determine whether the simulated vehicle could assume an attitude that allowed for it to maintain a condition of stable hovering flight without changing its position. To do so, instead of building an additional position controller, an optimization program was developed to resolve the previously defined equations under equilibrium conditions. This allowed to determine the trim, hovering attitude and actuation inputs of both the Mini-E and test vehicle tri-rotors. These studies were performed not only for ideal, no gust conditions, but also for a range of gust speeds hitting the vehicle from various directions.

These trim studies allowed to draft an initial hovering flight envelope where the maximum magnitudes of the gusts for each direction were computed for both vehicles as for them not to surpass some defined limits in terms of attitude and actuation. These limits (LB - Lower Bounds; UB - Upper Bounds) are depicted on Table 2.

Table 2: Study variables' boundaries.

Variable	**LB**	**UB**
ϕ	$-30°$	$30°$
θ	$-30°$	$30°$
Ω_1	$0\,rpm$	$8200\,rpm$ / $38400\,rpm$
Ω_2	$0\,rpm$	$8200\,rpm$ / $38400\,rpm$
Ω_3	$0\,rpm$	$6374\,rpm$ / $16640\,rpm$
δ_{arms}	$-15°$	$15°$
δ_r	$-30°$ / NA	$30°$ / NA
	(Mini-E / Test vehicle)	

As for the flight envelopes determined, the limit values found are available on Table 3 with the maximum gust speed magnitude simulated for each direction being $10m/s$. Despite the vehicles being able to withstand magnitudes above this value for certain directions, namely the test vehicle, due to not having any lifting surfaces and a relatively small airframe, rendering it less susceptible to being influenced by gusts, it was considered that this should be the upper limit. This value is greater than the maximum allowed gust magnitude currently used during flight testing of the current iteration of the Mini-E aircraft.

Table 3: Maximum allowable gust magnitude in each direction.

Gust Direction	**Maximum allowable magnitude (m/s)**	
	Mini-E	***Test vehicle***
Front	>10	>10
Rear	>10	>10
Left	4	9
Right	4	>10
Up	7	>10
Down	4	>10

When it comes to the attitude and actuation in-

puts required to achieve stable hovering flight in a gust free environment, the values obtained are provided on Table 4.

Table 4: Values of the different optimization variables in trim conditions for both aircraft.

Variable	Mini-E	Test Vehicle
ϕ	$-0.338°$	$-0.700°$
θ	$0°$	$0°$
Ω_1	$6047\,rpm$	$21995\,rpm$
Ω_2	$6047\,rpm$	$21995\,rpm$
Ω_3	$4909\,rpm$	$11222\,rpm$
δ_{arms}	$2.484°$	$5.019°$
δ_r	$0°$	NA

While the rotor actuation inputs (rotational speeds) are dependent on the propulsive system used (Propeller-Motor-ESC), a tendency in the attitude and frontal arms rotation angle can be deducted from the results shown. It was found that, for both vehicles, and under hovering conditions, the drag torque developed by the rear rotor was higher than the one developed by the two front rotors combined. This meant that the overall moment due to the drag torques was negative in the z direction of the referential shown on figure 1 and that the front rotors will, for both aircraft, be required to tilt to the right (thus the positive values of δ_{arms}) in order to develop a positive torque in z that balances the accumulated drag torques. This is achieved by creating a positive y thrust component that, in order to prevent the aircraft from drifting to the right, requires balancing. This balance is achieved by assuming a negative roll angle which results in a negative y component of the gravitational force to arise, thus balancing the forces in y.

Apart from these studies, an investigation on the influence of the rear rotor's tilting angle on the forward speed achieved by the aircraft was also done. To do so, the equilibrium equations were solved for different values of frontal gusts (simulating the aircraft's forward speed) and the rear rotor's tilting angle required to achieve equilibrium at each speed was obtained. With μ being taken as an additional design variable, the pitching angle was fixed at $0°$. This allowed to understand how the rotational speed of the rotors, frontal arms tilting angle, roll angle and rear rotor tilting angle would progress with the increase in the aircraft's forward speed. This investigation was done for both vehicles with different objectives. While for the Mini-E this investigation allowed to gain an initial understanding on the conditions required to transition between vertical and horizontal flight, for the test vehicle, which can not perform a transition due to not having any lifting surfaces, this study had the objective of determining whether it would be possible to perform forward flight through this tilting action and, if so, how the tilting angle would relate to the forward speed gained.

A graphical representation of the relation between the tilting angle of the rear rotor and forward speed is available in Figure 3 for the case of the Mini-E aircraft with a tri-rotor configuration.

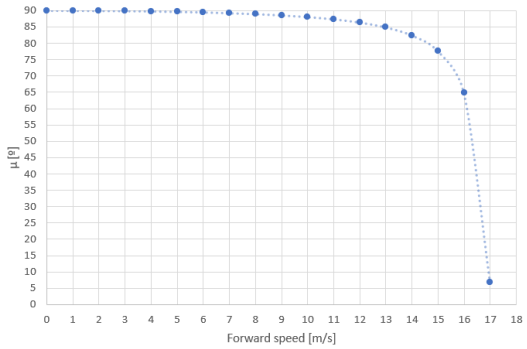

Figure 3: Evolution of the rear tilting angle, μ, with forward speed.

From these results it becomes clear that, in the vicinity of $\mu = 90°$ (rear rotor shaft in a vertical position), very fine adjustments to the tilting angle will generate considerable variations in the forward speed and that, to attain a flight speed of approximately $13\,m/s$ (stall speed of the aircraft), it would only be necessary to tilt the rear rotor by $5°$. After this stage, the variations in the tilting angle necessary to increase the flight speed will become larger as the aircraft's lift generation will stop depending mainly on the thrust developed by the rotors (which slow down in the process) and starts depending primarily on the lift force generated by the lifting surfaces, thus allowing for the rear rotor to tilt further and start providing mostly horizontal thrust.

3.4. PixHawk® Controller Implementation

In order to achieve the stabilization and control required to fly this novel configuration, the $PixHawk®$ 4 board [14] was elected running the $PX4$ flight controller firmware [15].

In spite of the PX4 autopilot firmware having two, pre-defined, tri-rotor airframes available for use, those could only be applied to tri-rotors with a "Y" configuration where the three rotors are equal in characteristics and equidistant from the aircraft's CG, thus equally loaded. Furthermore, in these setups, only one rotor (the rear one) is able to tilt laterally as to manage the yaw attitude of the aircraft, instead of the two front rotors as in the proposed design. Therefore, a custom PX4 airframe which incorporated the specific design of the proposed configuration needed to be defined. To do so,

custom geometry and configuration files were defined, as well a a custom mixer matrix file, which specifies the influence of the various actuators upon the different attitude axis and vertical thrust developed by the aircraft. In order to avoid coupling between the yaw axis actuation and the pitch attitude of the vehicle (due to the sense of rotation defined for the different propellers), the authority over yaw was attributed solely to the frontal rotors' tilt mechanism in a way that the autopilot does not resort to the usual strategy of changing the rotational speed of specific rotors to generate a yawing torque as usually done in other multi-rotor vehicles.

The custom autopilot firmware which was obtained was then flashed onto the *PixHawk®* 4 board through *QGroundControl* [16],

4. Airframe and Systems Sizing

4.1. MTOM Assumptions

To begin the sizing of the test vehicle, an initial MTOM value needed to be estimated in order to serve as a target for the sizing of the propulsive system and throughout the design of the different subsystems. As so, the masses suggested on Table 5 were taken as reference.

Table 5: Initial mass estimation.

Subsystem	**Mass (g)**
Airframe	100
Tilt mechanisms	500
Battery	200
Electronics	300
Total	1100

4.2. Procurement of motors, propellers and ESCs

From the suggested MTOM value, and under hovering conditions, each front rotor will be responsible for managing around 10% of the overall weight whereas the rear one will carry 80%. As so, the components enlisted on Table 6 were chosen for the propulsive system. The main choice criteria was the performance provided by each motor-propeller-ESC group (namely maximum thrust) when used alongside a 4S battery. Furthermore, availability in the workshop or in local suppliers was also taken into consideration.

Table 6: Propulsive system components.

	Front Rotors	**Rear Rotor**
Motor	iFlight XING 1404 3000 KV	iFlight XING 2806.5 1300 KV
Propeller	Gemfan 4024-2	Gemfan 7040-3
ESC	T-Motor Air 20A	T-Motor T80A

As referred earlier, these parts were chosen to work alongside a 4S battery (1600 mAh) due to availability of said battery model in a relatively large quantity in the workshop while providing, according to the components' manufacturers datasheets, appropriate performance both in terms of available thrust and flight time, which was estimated at around 3 minutes and 46 seconds in hovering conditions.

4.3. Airframe

The airframe of the test aircraft was designed and built using a combination of balsa and plywood. These materials were chosen due to the fact that they were inexpensive, easy to process, to repair, compatible and allowed for obtaining a light but strong frame while being available immediately.

4.4. Tilt mechanisms

4.4.1 Front mechanism

The frontal tilt mechanism allows for the rotation of the tri-rotor's arms along their respective axis as to perform a vectoring action of the front rotors' thrust, thus producing a lateral component that allows for the control of the aircraft's attitude in yaw while still providing enough vertical thrust for the aircraft to maintain altitude and be manoeuvred around the remaining axis. Special attention was given when sizing said arms in order to minimize their deflection under load, thus ensuring that the commanded thrust vectoring action occurs without deviations. Furthermore, an analytical assessment of the magnitude of the stresses that would be imposed onto said structure was also done, with the results yielding that, under normal operating conditions, the structural integrity of the system was assured. The CAD representation of said subsystem is available in Figure 4.

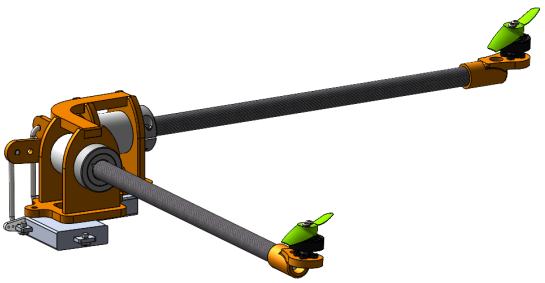

Figure 4: Front tilt mechanism CAD.

4.4.2 Rear mechanism

Despite not acting as a primary control actuator in vertical flight conditions, and even though its tilting capabilities will not be fully explored in this experimental vehicle as would happen in a fixed wing, VTOL, aircraft, it was deemed necessary to model the complete rear tilting mechanism. As so,

and even though an electric motor was used, it was decided that this should be mounted in a similar way as would happen with the internal combustion engine of the final aircraft. This allowed to study the effects that the introduction of a 90° gearbox into the propulsion system has on the overall performance of the system as well as to perform forward flight testing through the tilting action of this rear propeller (even though limited for obvious reasons). The CAD representation of said subsystem is then available in Figure 5.

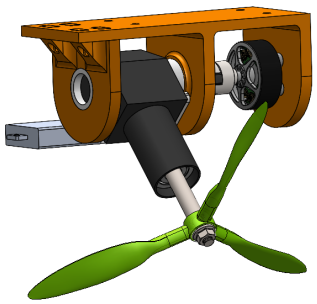

Figure 5: Rear tilt mechanism CAD.

4.5. Experimental testing and results

4.5.1 Thrust tests

In order to validate the choice of motors, propellers and ESCs when it comes to thrust provided and to obtain other data such as consumed power or torque developed, which were necessary to further develop the computational model of the aircraft, static thrust test were conducted. As so, both the front and rear propulsive systems (ESC-Motor-Propeller) were tested in direct drive, with the propeller mounted on the motor shaft, and later, after the rear tilting mechanism was built, the rear propulsive system was tested once more. This last test was done with the purpose of comparing the difference in electrical power consumption that arises from the introduction of the 90° gearbox between the motor shaft and the output shaft on which the propeller is mounted, while providing a similar thrust figure as in direct drive. This allowed to study the loss in efficiency of the final assembly in relation to the default, direct drive, setup and to relate it with the usual efficiency curves found in the literature for various types of gearboxes.

Table 7: Thrust testing results.

Propulsive System	Maximum thrust (exp.)	Thrust Margin
Front	331 g	66.8%
Rear	1147 g	23.3%

On Table 7 some relevant information regarding the maximum thrust figures obtained from said tests and the thrust surplus in relation to the value required from each rotor in hovering conditions are provided. Furthermore, Figure 6 presents the graphical representation of the *Power vs Thrust* curves for both direct drive and complete rear rotor tilting mechanism as well as the loss of efficiency curve, which is coherent with gearbox efficiency curves obtained by other authors [3, 4, 6]. From the results shown, the loss in efficiency under hovering conditions will be of around 19%.

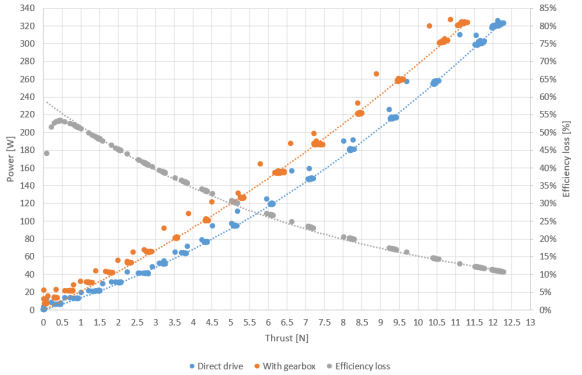

Figure 6: Power vs thrust curves for direct drive and for the entire rear tilting mechanism and loss of efficiency curve.

After these static thrust tests were performed, continuous operation testing took place, where the rear propulsive system was requested to operate with 80% throttle (slightly above hovering conditions) for 30, 60 and 120 seconds in order to assess the evolution in the motor and gears temperature and also the thrust output evolution with time. It was found that during the first $35s$ of operation a drop in thrust ($9.75\,N$ to $9.2\,N$) was verified alongside a temperature increase in the electric motor. However, after the $45s$ mark both values stabilized, with the motor reaching a final temperature of $78°C$ (well bellow the maximum operating temperature of $105°\,C$ achieved during static thrust testing with a 24V input voltage according to the manufacturer).

4.5.2 Actuator mapping

After both tilting mechanisms were assembled, their mapping was done using a PWM generator and a digital angle gauge. This allowed to update the computational model of the vehicle's actuation, particularly of the front tilt mechanism (Figure 7). A trade-off was made during the assembly of the rear mechanism in order to enhance the resolution of the angle adjustment near the vertical position in detriment of having the ability to tilt the propeller shaft to a fully horizontal position, which would

bring no benefits to the test vehicle's operation anyway.

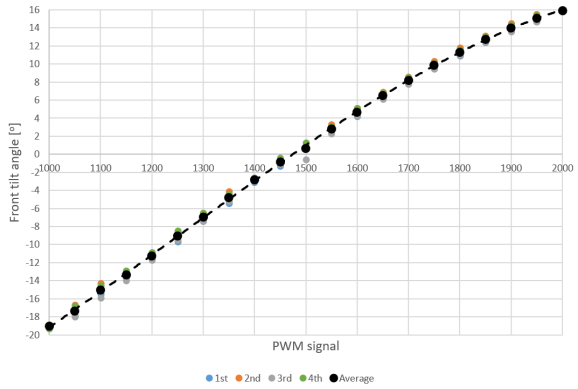

Figure 7: Mapping of the front tilt mechanism actuation.

With all of the subsystems built and tested it was then possible to mount them onto the airframe. The final complete assembly weighed in at 1168 g, 6% over the initial estimation. Given the thrust surplus registered on Table 7, this MTOM value was deemed acceptable.

5. Flight Testing

5.1. Hovering flight and autopilot tuning

Due to the experimental character of the test vehicle developed, it was required to take special security measures at the beginning of the flight testing phase. As so, the first set of test flights were performed indoors and with the aircraft tethered to four 5 kg weights. These initial flights were done with the objective of tuning the autopilot and the aircraft itself and also for the test pilot to be familiarized with the vehicle's dynamics. As so, three tethered tests were done with sequentially increasing slack being provided to the tethers as the vehicle stability and manoeuvrability was improved. By the time of the third tethered flight the vehicle was already controllable, with minimal trim being required to fly it in a way that it was possible to perform the first, indoor, untethered flight (Figure 8). During this test the vehicle proved capable of achieving steady hovering flight and to perform manoeuvres in all axis.

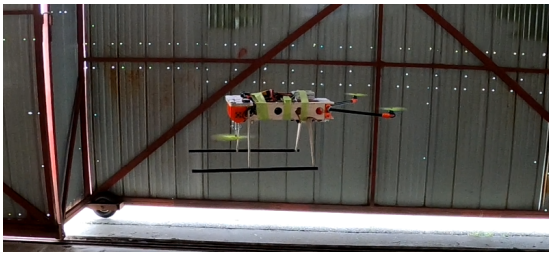

Figure 8: Indoor flight without tethers.

After this successful test, it was then possible to proceed to outdoor testing where the aircraft showed once more that it could sustain stable hovering flight and carry out manoeuvring across all axis even when exposed to real world conditions and in the presence of wind gusts. With this, it was considered that the proposed aircraft configuration was airworthy.

5.2. Forward flight

Once the airworthiness of the vehicle was proved, a test flight where the rear rotor was tilted by 5° was performed (Fig. 9). Although the rear tilting mechanism is not used by the autopilot as a control actuator, an auxiliary control channel was programmed to allow for the pilot to introduce the tilting angle mentioned above. As so, after achieving stable hovering flight, the rear propeller shaft was tilted by 5°. The aircraft showed a considerably stable attitude, being able to gain forward momentum while maintaining a leveled attitude. After 6s, due to test perimeter restrictions, the pilot reverted the rear tilt angle to 0° and proceeded to land the aircraft. This test proved the ability of the proposed concept to initiate and perform forward flight, paving the way for future transition condition studies to be made.

Figure 9: First outdoor forward flight.

5.3. System identification flights

An additional set of test flights was performed with the objective of collecting the flight data needed to perform system identification of the developed vehicle. These flights were required to include sets of specific manoeuvres meant to excite certain dynamics of the aircraft, namely *doublets* and *chirps* (or *frequency sweeps*). As so, and following pre-developed test procedures, four flights were made. The first three tests where dedicated to each of the three attitude axis, in a way that in each flight, from start to finish, only one axis was excited. Finally, in the fourth test, the validation flight, the pilot requested *doublets* and *chirps* in all axis (one at a time). This last flight was later used to validate the models obtained from system identification.

6. System Identification

After the data gathering flights were conducted, the information contained in the *log* files was pro-

cessed in a way that it could be fed to the two algorithms meant to be used to perform system identification of the developed vehicle.

6.1. Time based approach

The first objective of this SID step was to validate the previously derived FDM against experimental results. As so, a Simulink model of the vehicle was developed using the equations obtained and where a number of design parameters were taken as variables. A cost function block was also added to this Simulink model, where the simulated dynamics were compared to the ones registered during flight testing. This model was then linked to an optimization tool which, given an initial estimation of said design variables (acquired during ground testing or during the initial design phase), would explore the design space, varying these values in such a way that the cost function was minimized, i.e., that the behaviour of the simulated vehicle was as similar as possible to the one of the real vehicle during the test flight. In total, 42 design variables were explored.

In order to reduce the initial computing cost of such program, small time intervals of $0.5s$ were initially introduced, with these being increased gradually. However, it was found that for time intervals over $2s$ the simulated dynamics would diverge from the registered ones and that the program showed a tendency to assume very small variations of the design variables in relation to the initial points that were provided, yielding that those were already associated to a local minimum in the cost function. In order to add flexibility to the model, various initialization times were provided, with the algorithm showing a similar behaviour irrespective of the starting time. However, this diverging tendency was not entirely unexpected when considering the natural bare-airframe instability that is a characteristic of most rotorcraft configurations, being, in fact, mentioned in the literature [17]. Said literature also advocates for the use of frequency-response techniques, which are prone to provide more satisfactory results at a lesser computational cost when dealing with the task of performing system identification of rotorcraft.

6.2. Transfer-function approach

In order to obtain a dynamics model capable of replicating the aircraft's dynamics, through a frequency-response technique, a transfer-function approach was then chosen. The two main drawbacks of this method are: 1) Although being a parametric approach, it does not provide insight into the validity of the physical FDM previously obtained against the real vehicle as the only values obtained are the coefficients of the numerators and denominators of the transfer-functions which provide the ratio of the response per unit of control input; 2) It provides a linearized model where the changes in attitude for a given axis (rates) are solely related to the input (rate setpoints) provided for that same axis, neglecting coupled dynamics.

Nevertheless, it is of interest to apply said method to the collected data as it will allow to obtain an experimental-based dynamic model which can be used, for example, for autopilot tuning. As so, a custom Matlab algorithm was used. This program received data from the three, individual axis, SID flights, alongside an array of timeframes related to the temporal location of the manoeuvres performed in the data files. Then, the program would arrange combinations of these timeframes and perform an estimation of the transfer-function which best related the inputs and the outputs for that combination of manoeuvres. After this, the various transfer functions obtained would be applied to the validation flight's inputs for their respective axis and the one which presented the best fitment between its outputs and the ones registered in the real flight would be chosen. The goodness of fitment values for the three transfer-functions which were obtained, when applied to the validation flight are presented on Table 8.

Table 8: Frequency-response SID results.

Axis	**Goodness of fitment** [%]
Roll	79.57
Pitch	67.62
Yaw	62.04

These results, even though satisfactory and appropriate for the aforementioned use in autopilot tuning, are quite harmed by the coupled dynamics of the test vehicle, mainly when it comes to the yaw axis, where, for example, pitch manoeuvres will cause oscillations in yaw (as the inclined front rotors have their rotational speed varied during such manoeuvres) which, with no input being provided in yaw, will not be reflected by the model, reducing the fitment. Nevertheless, the replication of manoeuvres effectively requested for a given axis is quite good and the model is able of adequately replicating the full flight. This method, by requiring only one flight per axis to gain information on the dynamics of the vehicle (alongside an additional validation flight) allows for a low turnaround time to acquire a dynamic model with quite satisfactory results, specially for vehicles with less coupled dynamics than the presented tri-rotor.

7. Conclusions

The main goal of the presented work was to prove the airworthiness of the proposed conceptual tri-

rotor configuration. This goal was successfully met, with the developed test vehicle managing not only to achieve stable hovering flight in real world conditions (in the presence of gusts) but also to perform various manoeuvres with varying frequencies in all axis. Moreover, the vehicle proved capable of performing stable forward flight, as would be required in the transition phase of a VTOL fixed wing aircraft, paving the way for future transition condition studies to be made.

Furthermore, a successful development of a preliminary Flight Dynamics Model was verified, with several trim studies being carried out and many of the results obtained validated during the following flight testing phase. Moreover, it was possible to derive a dynamics model from the data that was gathered during testing by means of a frequency-response SID algorithm.

The presented work may be continued by applying other SID tools to the collected data (such as $CIFER^{®}$ [17]) in order to further validate the physics based FDM that was developed throughout this investigation. Furthermore, and before the development of the final iteration of the Mini-E vehicle (tri-rotor), a trade-off study should be performed as to determine whether the final aircraft should have its rear rotor directly powered by an ICE, as proposed, or through a tilting electric motor (without gearbox and the associated losses) powered by a series hybrid system. This study should aim, once more, at the maximization of the aircraft's range.

References

[1] E. M. Almas. Course notes, Machine Elements. Department of Mechanical Engineering, IST, 2020. Accessed on 2022-05-07.

[2] N. E. Anderson and S. H. Loewenthal. Effect of Geometry and Operating Conditions on Spur Gear System Power Loss. *Journal of Mechanical Design*, 103(1):151–159, Jan. 1981.

[3] B. Clavac and Z. Korka. Efficiency investigation on a helical gear transmission. *Analele Universităţii "Eftimie Murgu" Reşiţa, Fascicola Inginerie*, XXIV:pp. 55–66, Oct. 2017.

[4] N. Goudarzi and W. Zhu. Studying the potential of a novel multiple-generator drivetrain in wind energy conversion systems. Volume 4B: Dynamics, Vibration and Control, Nov. 2013.

[5] F. Lopot, M. Dub, J. Flek, D. Hadraba, M. Havlíček, L. Kučera, O. Štoček, T. Veselỳ, and J. Janáček. Gearbox mechanical efficiency determination by strain gauges direct application. *Applied Sciences*, 11(23):11150, 2021.

[6] K. Michaelis, B. R. Hoehn, and M. Hinterstoißer. Influence factors on gearbox power loss. *Industrial Lubrication and Tribology*, 63:46–55, Feb. 2011.

[7] R. P. Sekar. Determination of load dependent gear loss factor on asymmetric spur gear. *Mechanism and Machine Theory*, 135:322–335, 2019.

[8] F. Wang, X. Xu, J. Xia, and H. Que. Effect of tooth surface modification on dynamic transmission efficiency of double helical gear trains. *International Journal of Acoustics & Vibration*, 26(4), 2021.

[9] G. Ionascu, C. Rizescu, L. Bogatu, L. A. Cartal, and E. Manea. Study of influence of surface microtexture and roughness on friction coefficient. *DEStech Transactions on Engineering and Technology Research*, May 2017.

[10] R. M. Wang, S. R. Zheng, and Y. P. Zheng. 11 - other properties of polymer composites. In R. M. Wang, S. R. Zheng, and Y. P. Zheng, editors, *Polymer Matrix Composites and Technology*, Woodhead Publishing Series in Composites Science and Engineering, pages 513–548. Woodhead Publishing, 2011.

[11] D. Tomás. Design, development and manufacture of a new vtol, canard uav. Master's thesis, Instituto Superior Técnico, Dec. 2020.

[12] S. Pedro. Sizing and integration of an electric propulsion system for a vtol uav. Master's thesis, Instituto Superior Técnico, Dec. 2020.

[13] J. Oliveira. Apontamentos de estabilidade de voo. Department of Mechanical Engineering, IST, 2018. Accessed on 2022-03-23.

[14] Holybro. Pixhawk 4, May 2018. URL `http://www.holybro.com/product/pixhawk-4/`. Accessed on 2022-05-17.

[15] Dronecode Foundation. PX4 Autopilot. Online. URL `https://px4.io/`. Accessed on 2022-05-17.

[16] Dronecode Project. QGroundControl. Online, 2019. URL `http://qgroundcontrol.com/`. Accessed on 2022-05-17.

[17] M. B. Tischler and R. K. Remple. *Aircraft and Rotorcraft System Identification - Engineering Methods with Flight Test Examples*. American Institute of Aeronautics and Astronautics, Inc., second edition, 2012. ISBN: 978-1-60086-820-7.